1-21-2013

Rapid generation and manipulation of microfluidic vortex flows induced by AC electrokinetics with optical illumination

Choongbae Park
Purdue University, choongbaepark@purdue.edu

Steven T. Wereley
Birck Nanotechnology Center, Purdue University, wereley@purdue.edu

Park, Choongbae and Wereley, Steven T., "Rapid generation and manipulation of microfluidic vortex flows induced by AC electrokinetics with optical illumination" (2013). *Birck and NCN Publications.* Paper 1315.
http://dx.doi.org/10.1039/c3lc41021h

Lab on a Chip

RSC Publishing

PAPER

View Article Online
View Journal | View Issue

Cite this: *Lab Chip*, 2013, **13**, 1289

Rapid generation and manipulation of microfluidic vortex flows induced by AC electrokinetics with optical illumination†

Choongbae Park and Steven T. Wereley*

Received 8th September 2012,
Accepted 21st January 2013

DOI: 10.1039/c3lc41021h

www.rsc.org/loc

We demonstrate a rapid generation of twin opposing microvortices (TOMVs) induced by non-uniform alternating current (AC) electric fields together with a laser beam on a patterned pair of indium tin oxide (ITO) electrodes. A fast and strong jet flow region between twin microvortices is also generated. Its pattern and direction, such as whether it is symmetric or asymmetric, are controlled mainly by the location of a single laser spot relative to the ITO electrodes. With two laser beams, two separate flows are superposed to give a new one. *In situ* generation and control of the TOMV flow are tested in suspensions of fluorescent polystyrene particles, as well as in milk emulsions. This technique has great potential for dynamically manipulating micro-fluid flows, functioning as a micro-pump or mixer.

Introduction

It is always challenging to generate a desirable flow in a microchannel for delivering, sorting, and mixing, as well as to control the motion of particles. Fast and easy generation of micro-fluid flow and its control have always fascinated the researcher for handling biological and chemical samples. Electrokinetic methods provide advantages over the conventional methods, *i.e.*, mechanical pumps, since they have no moving parts, reducing fouling problems. Many approaches using AC electrokinetic techniques, such as alternating current electrothermal (ACET) and AC electroosmotic (ACEO) flows, have been developed to not only generate fluid flow but manipulate particles in fluid. Usually, microflows generated by using a pair of symmetric electrodes are counter-rotating vortices in a plane perpendicular to the plane where two electrodes are placed.[1–3] In order to make a unidirectional flow, more complicated techniques such as asymmetric electrodes array,[4] 3D electrode array,[5] T-shaped electrodes[6–8] are often used. At the same time, dielectrophoretic (DEP) effect on particle manipulation by using several different shapes of electrodes have also been studied.[1,9–11] Instead of metal electrodes, an optically patterned electrode, *i.e.* a partially illuminated area on an ITO film or a photoconductive material, is used to assemble and manipulate particles on the electrode.[12,13]

On the other hand, a highly focused laser beam by itself can trap and manipulate individual particles, such as optical tweezers.[14,15] Recently, however, lasers have been used with AC electric fields to generate vortical flows employing a highly focused infrared (IR) beam.[16,17] Similar experiments have been replicated on parallel-plate ITO electrodes and planar interdigitated ITO electrodes, and toroidal microvortices as well as microvortices similar to four roll mill flow have been studied.[18–20] Nevertheless, relatively little information exists on manipulating and controlling microfluidic flows using this technique, even though it has already been used for specific applications such as stretching DNA molecules.[21] With two coplanar electrodes, vortex flow was generated when the laser spot was located between two electrodes[16,21] or adjacent to the electrode,[17] while vortex flow was observed by locating the laser spot on one of interdigitated ITO electrodes.[20] In addition, those techniques required relatively high-frequency, high-voltage AC signal and a highly focused laser beam, and their flows were limited to one type of flow which is similar to the flow in four-roll mill device.

In this article, we demonstrate microfluidic generation of twin opposing microvortices (TOMVs) and manipulation of fluid flow in a single hybrid opto-electrofluidic platform which combines a moderately focused laser beam with AC electric fields generated by two coplanar ITO electrodes. Various shaped flows with TOMVs are generated by changing the location of a laser spot on the ITO electrode in a microchannel. Two laser beams applied simultaneously produce a different shaped flow such as superposition of two separate flows.

Birck Nanotechnology Center and School of Mechanical Engineering, Purdue University, West Lafayette, IN 47907, USA. E-mail: wereley@purdue.edu; Fax: +1-765-494-0539; Tel: +1-765-494-5624

† Electronic supplementary information (ESI) available: Supplementary figures and movies. See DOI:10.1039/c3lc41021h

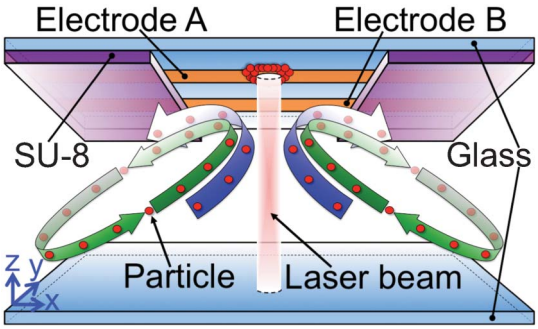

Fig. 1 Schematic illustration of the TOMV flow with two opposing microvortices (green circular arrows) and jet flows (blue curved arrows) generated by a laser illumination and two coplanar ITO electrodes A and B on the upper surface of the microchannel. Particles (red circles) are moving in the plane which is slightly inclined to the horizontal plane (*i.e.*, the *x*–*y* plane). The direction and shape of the arrows represent the flow generated by the laser spot location shown above (*i.e.*, at the middle of exposed electrode A) under non-uniform AC electric fields from the two exposed electrodes. Note that all following images show the projected motion of particles in the horizontal focal plane. In addition, schematic illustrations of the non-uniform electric field lines and the experimental setup can be found in Fig. S1 and S2†, respectively.

Materials and methods

In this device shown in Fig. 1, two electrodes A and B on the upper surface of the microchannel were fabricated from a glass substrate uniformly coated with an ITO of 500 nm (SPI Supplies, West Chester, PA, USA). Standard soft lithography and a wet etching technique were used to pattern the ITO film. The width of each electrode was 16 μm, and the distance between two ITO electrodes was 73 μm. In order to define an exposed portion of the electrodes, SU-8 negative photoresist was used to cover the unwanted area of ITO electrodes, so that a small portion of the ITO electrodes having a length of 300 μm was exposed to the fluid. The role of SU-8 film is to weaken, possibly block, non-uniform AC electric fields generated by two ITO electrodes, which could confine the electric fields in a specific region inside the microchannel. Also, the patterned SU-8 film made a rectangular groove on the upper surface of the microchannel. Finally, the other bare glass substrate was bonded with the ITO electrode glass substrate by using a two-sided adhesive tape (Adhesives Research Inc., Glen Rock, PA, USA) as a spacer (25.4 μm thick) which defined the height of the channel in addition to SU-8 film (6.33 μm thick). 1 μm red fluorescent polystyrene particles (1% solids) purchased from Thermo Scientific were used for tracing the flow. It was diluted to 0.014% with the DI water in order to have proper number of particles in a region of interest to perform micro-particle image velocimetry (μPIV).[22] Further experiments were done with commercially available milk to confirm that this technique could be extended to manipulate emulsions, as well as to investigate the fundamental physical mechanism underlying twin opposing microvortex generation.

The laser beam was positioned on the exposed ITO electrode using an inverted microscope equipped with a Nd:YVO4 laser illumination system, Bioryx® 200 (Arryx Inc., Chicago, USA) which generates multiple laser spots or patterns using a spatial light modulator, or SLM.[15] An AC signal was applied between two electrodes up to 10 Vp–p (peak-to-peak voltage) and 2.0 MHz while the laser power was fixed. The voltage and frequency of the AC signal were kept constant when varying the applied laser power up to 1.2 W. Regions of interest on two microvortices around the exposed electrodes were imaged by a Foculus IEEE 1394 Digital CCD camera. The side walls of the microchannel were located at least 970 μm away from the exposed ITO electrode along the *x*-axis, and the length and width of the microchannel constructed by the adhesive tape were about 8400 μm and 2780 μm, respectively, while the region of interest on the upper surface of the microchannel, parallel to the *x*–*y* plane, including two ITO electrodes exposed to fluid was about 300 μm × 105 μm. Thus, the influence of the spacer on vortex flow could be neglected, since strong and stable vortices occurred only around the exposed electrode region whose area was relatively small compared to that of whole microchannel. In addition, the moving particles did not touch or collide with the upper and bottom surfaces of the microchannel (including SU-8 structures), which was confirmed by the comparison of particles fixed on the upper and bottom surfaces with moving particles by focusing and defocusing them.

Results and discussion

Experiments are conducted by shining the laser beam onto one of the exposed ITO electrodes while applying an AC signal between them. When the laser spot is on any region of the

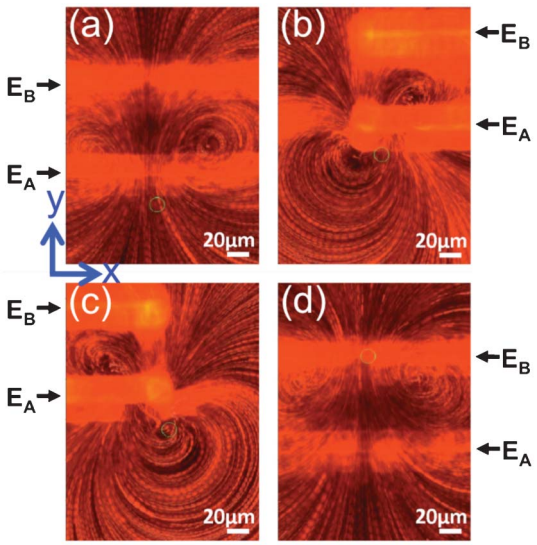

Fig. 2 Overlapped images showing various microvortex flows according to the location of the laser spot on two exposed ITO electrodes A and B (E_A and E_B, respectively). The laser spot is at the middle (a), left edge (b), right edge (c) of exposed electrode A, and (d) middle of exposed electrode B. Note that each overlapped image was made of 50 consecutive frames from the recorded movies (supplementary movie 2 and 3, ESI†).

exposed ITO electrode, a rapid opto-electrokinetic vortex flow is generated. (see Fig. 1 and 2, and supplementary movie 1, ESI†) When the particles are moving near the laser spot, they move very fast near the top of the microchannel (*i.e.*, close to the upper surface of the microchannel), whereas in other cases, they move slower near the bottom. Its motion is a complex, three-dimensional vortex flow but remains steady in time. The flows are observed in an imaging area of 236.8 μm × 177.6 μm and viewed from the bottom (*i.e.*, the *x*–*y* plane). The in-plane dimensions are relatively large compared to the maximum height of the microchannel (H = 32.23 μm), and thus the two-dimensional particle motion is projected on the measurement plane perpendicular to the *z*-axis. This flow is characterized by "twin opposing microvortices" (TOMVs) which are steady-state symmetric counter-rotating microvortices. Between these twin microvortices, a "jet flow" region in which straight, hyperbolic or parabolic streamlines exist is also observed, and the center of each microvortex seems to originate from the region between two electrodes, even more specifically, close to the electrode on which the laser beam shines. It is also observed that the twin microvortex flow starts to be generated at about 1 kHz when ramping up only frequency from 0 Hz at a fixed voltage of 9 Vp–p while applying the laser power of 0.5 W. When the fixed voltage is changed to 5 Vp–p, the TOMV flow is generated at 70 kHz. Overall, the magnitude of velocity in the region outside two exposed electrodes reaches up to 53.3 μm s^{-1} at the mid-plane between the upper and bottom surfaces of the microchannel, *i.e.* at $z = h/H = 0.48$ where h is the distance from the bottom surface to the focal plane along the *z*-axis, under the conditions: 107 kHz and 9 Vp–p of AC signal, and 0.5 W of laser power. The fluid velocity in the jet flow region, especially close to the laser spot, is much faster than that in the rest of the microchannel, since the strongest interaction of AC electric fields and laser illumination is expected to occur there. Thus, it is estimated the flow field around the laser spot have a velocity of at least 2–3 times the maximum velocity in the region outside the exposed electrodes by tracking the particle trajectories.

The underlying mechanism of the TOMV flow can be understood by considering the case of two coplanar electrodes without an external illumination in which the time average electric force ($\mathbf{f}_E$) acting on the fluid is given by[3]

$$<\mathbf{f}_E> = \frac{1}{2}\mathrm{Re}\left[\frac{\sigma\varepsilon(\alpha-\beta)}{\sigma+i\omega\varepsilon}(\nabla T\cdot\mathbf{E}_0)\mathbf{E}_0^{*} - \frac{1}{2}\varepsilon\alpha|\mathbf{E}_0|^2\nabla T\right] \quad (1)$$

where Re indicates the real part of the expressions inside brackets, σ and ε the conductivity and permittivity of the fluid, ω the applied frequency, $\mathbf{E}_0$ and $\mathbf{E}_0^{*}$ the electric field and its complex conjugate, T the temperature, $\alpha = \frac{1}{\varepsilon}\left(\frac{\partial\varepsilon}{\partial T}\right)$, $\beta = \frac{1}{\sigma}\left(\frac{\partial\sigma}{\partial T}\right)$. This equation shows that the character of fluid flow generated by this force varies greatly depending on the frequency and voltage of an applied AC signal, as well as temperature gradients causing changes in conductivity and permittivity of the suspending fluid.[23] In addition, fluid motion can be analyzed by considering only the two-dimensional flow on the vertical plane (*i.e.*, perpendicular to the length of the electrodes). In our case, however, an additional IR illumination onto the ITO electrodes along the *z*-axis shown in Fig. 1 will affect or alter the temperature gradients as well as electric field gradients compared to those generated only from the electrodes. Its induced fluid flow is consequently a three-dimensional motion but can be projected onto a two-dimensional *x*–*y* plane (*i.e.*, parallel to the plane including two electrodes) as explained above. The details of these phenomena described in the following sections will support this hypothesis with evidence from our experimental observations.

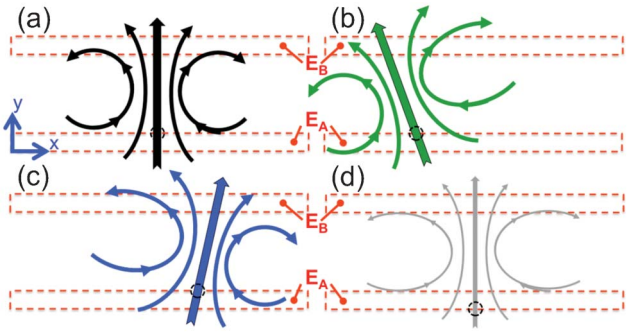

Fig. 3 Schematics of symmetric and asymmetric microvortex flows at various locations of the laser spot on an electrode: strong and weak symmetric flows at the middle-top (a) and middle-bottom (d) of exposed electrode A (E_A), respectively; asymmetric microvortex flows when the laser spot is moved to the left (b) and right (c) from its middle position shown in (a). (Red dashed rectangles and black dashed circles represent the exposed ITO electrodes and laser spot locations, respectively.)

There are six clearly recognizable representative flows which occur depending on the location of the laser spot on the two exposed electrodes (*i.e.*, at the middle, left edge, right edge of each electrode). Four of them are shown in Fig. 2 (see also supplementary movies 2 and 3, ESI†). In Fig. 2(a), when the laser spot is located in the middle of electrode A (referred to as E_A), the microvortices are generated near electrode A and the direction of jet flows is toward electrode B (referred to as E_B) (see also Fig. 3(a)). On the other hand, when the laser spot is moved to the middle of electrode B, the microvortices are generated near electrode B and the jet flow direction is reversed as shown in Fig. 2(d) (see also supplementary movies 2 and 4, ESI†). It is interesting to note that when the flow field in Fig. 2(d) flips across a "horizontal midline" that is midway between two electrodes, its flipped flow field is exactly the same as the one in Fig. 2(a). Moreover, the TOMV flow is symmetric with respect to a "vertical centerline" that passes through the laser spot between twin microvortices and is parallel to the *y*-axis. Note that this symmetric flow can be obtained only when the laser spot is exactly in the middle of exposed electrode A or B (this will be further discussed later).

Once the laser beam moves to the left or right from the middle of exposed electrode A or B, jet flows as well as twin microvortices are shifted in the same direction as much as the laser spot moves along the electrode. Simultaneously, the overall direction of the TOMV flow is gradually rotated in counterclockwise or clockwise direction (see Fig. 3(b) and (c)).

For example, when the laser spot is moved from the middle to the left on electrode A, the flow field is rotated in a counterclockwise direction shown in Fig. 3(b). In addition, symmetric flow with twin microvortices is changed to asymmetric flow, in which one vortex has a more elliptical (or elongated) shape than the other (see Fig. 3(b) and (c)), since the movement of the laser beam breaks symmetric electric and possibly thermal fields due to the combined effect of AC electric fields and laser illumination. Thus, the TOMVs are not perfectly identical to each other anymore. For example, the left vortex has a more elongated shape along the direction normal to jet flows as the laser spot moves to the right on electrode A (see Fig. 3(c)). As the laser spot gets close to the left or right edge of the exposed electrode, the rotation of the flow field is rapidly increased, and its maximum rotations were observed when laser spot was at both ends of exposed electrode A as shown in Fig. 2(b) and (c) (see also supplementary movie 3, ESI†). It is interesting to note, the centers of the left vortex in Fig. 2(b) and the right vortex in Fig. 2(c) are below electrode A in each case.

Once the laser beam falls into the region between two exposed ITO electrodes or moves away from them, the TOMV flow is not generated anymore (see supplementary movie 4, ESI†), even though ACET or ACEO flow due to only two planar electrodes is generated at a certain range of frequency and voltage.[3,24] But the magnitude of ACET or ACEO flow is relatively small compared to those from other groups, since the spacing between two electrodes is much larger than those[23,25] and thus weaker AC electric fields are generated.[2,24] Also, there is no obvious vortex flow when the laser beam shines on the ITO electrodes covered with SU-8 film. It was reported that SU-8 films transmit over 90% of 1064 nm light,[26] while ITO films absorb the irradiated IR laser energy.[27] Thus, it is very likely that the IR illumination electrically and/or thermally interacts with the unexposed ITO electrode as well. Nevertheless, there is no rapid vortex generation when the laser beam shines the ITO electrode through SU-8 film. This can be explained in two ways such as the electric field change and thermal heating due to an external illumination, which seem to be the key factors in generating twin opposing microvortices and jet flows. First, the electrical effects of the resultant interaction between the laser illumination and AC electric fields may be suppressed by SU-8 film, but not completely, since weak AC electric fields were observed in the SU-8 well.[28] This assumption is also supported by the fact that no particle aggregation on SU-8 film below the unexposed ITO electrodes occurs during the entire experiment. Secondly, SU-8 films are also good thermal insulators, thus it may prevent any heat transfer to the suspensions or the region of the exposed electrodes assuming that the IR illumination produces heating on an ITO electrode which is sandwiched between SU-8 film and glass substrate, since the thermal conductivity of SU-8 and glass substrate is much less than that of ITO electrode.[29–31] Moreover, it is noted that an amount of heat transfer along the *x*-axis may be negligible because the thickness of the ITO electrode is much smaller than its length and width.[3] Thus, the heating due to interaction between the unexposed ITO electrode and IR illumination is rarely transferred into the suspensions due to the SU-8 coating. Conversely, when the laser beam is shined on one of the exposed ITO electrodes while applying AC signal between two electrodes, these two factors, electrical and thermal effects, can explain the generation of the TOMV flow.

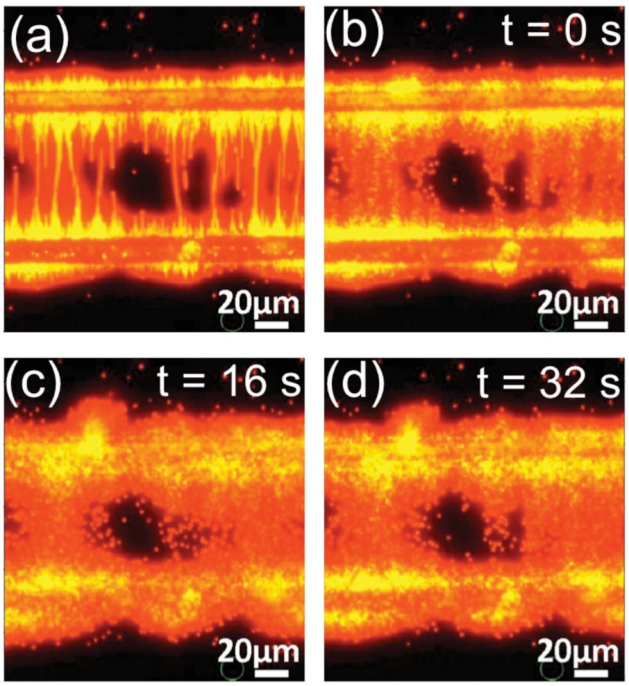

Fig. 4 Particle aggregation on the exposed ITO electrodes with no laser illumination. (a) Particles are collected on the exposed electrodes at 107 kHz and 9 Vp–p. (b)–(d) Consecutive images with an interval of 16 s after the voltage is decreased to 0.1 Vp–p while the frequency is kept constant.

When the illumination is switched off while AC signal at 107 kHz and 9 Vp–p is still applied, no microvortices are observed (see supplementary movie 1, ESI†). Instead, particles are collected on the edges of the exposed electrodes (*i.e.*, no particle aggregation on SU-8 film) as shown in Fig. 4(a). Positive DEP can explain this aggregation of particles because particles are collected in strong electric field gradient region.[1,32] Actually, this particle aggregation on the electrodes has been observed even if twin opposing microvortices are generated, since positive DEP is still the dominant force on the particles moving near the electrode at the upper surface of the microchannel. When the frequency of the AC signal is increased from 0.1 to a few hundred kHz, particles are collected on the electrodes at low frequencies on the order of tens of kHz (*i.e.* 5 kHz to 60 kHz), as reported by Ramos *et al.*[1] It is interesting to note, more particles are collected at the inner long edges of electrodes than the outer ones since the strongest electric field gradients are located at the inner edges of electrodes while the field gradients at the outer edges are somewhat weaker.[1] In addition, many particles are also attracted to the short edges of the exposed electrodes where

SU-8 film started to cover the unexposed part of the ITO electrodes. As time goes on without laser illumination, particles begin to slowly form pearl chaining along the width direction of the electrodes (*i.e.*, parallel to the *y*-axis), originating from both inner edges of electrodes, and a few of them finally meet each other bridging two electrodes. These particle chains can show the direction and magnitude of AC electric fields without laser illumination,[32,33] which shows that these electric fields are probably different from those of the TOMV flow. When the voltage is decreased down to 0.1 Vp–p, the collected particles begin to spread out on a longer time scale in comparison to the TOMV flow, showing Brownian motion of particles in suspensions as shown in Fig. 4(b)–(d).

These opto-electrokinetic microvortex flows generated by various locations of the laser beam on one of two electrodes can be categorized into four types of flow fields: strong and weak symmetric flows according to the location of the laser spot in the direction of the *y*-axis (Fig. 3(a) and (d)), and asymmetric flows with counterclockwise and clockwise rotation due to the movement of the laser spot along the *x*-axis (Fig. 3(b) and (c)). Note that these four flow fields can be obtained on either electrode A or B, because the TOMV flow can be reversed across the horizontal midline between two electrodes. When the laser spot gets close to the top edge of electrode A along the *y*-axis, a strong microvortex flow is generated (Fig. 3(a)), while a weak one is obtained when the laser spot is moved to the bottom edge (Fig. 3(d)). The magnitude of the overall velocity of the weak flow is much smaller than that in the strong one, and the vortex shape of the weak flow becomes more elliptical in contrast to that of the strong one, because weaker AC electric fields at the bottom edge of electrode A[1] also alter, *i.e.* reduces, the influence of the combined effect between the AC electric fields and laser illumination on the flow field.

This opto-electrokinetic technique can also be applied to manipulate milk emulsions obtained from commercially available 2% milk. All the different flow fields as well as twin opposing microvortices generated in DI water suspensions of polystyrene particles have been successfully reproduced in milk emulsions. Here, another flow can be generated by using two holographic laser beams in milk emulsions (see supplementary movie 5, ESI†). Note that this movie is rotated 90 degrees in clockwise direction regarding to Fig. 5.). If only one laser beam is applied on either side of exposed electrode A, the rotated flows shown in Fig. 5(a) (top and middle) are generated, and its corresponding overlapped images are shown in Fig. 5(b) and (c), respectively. Once two laser beams are simultaneously applied on the same spots as the previous cases, a new flow is generated by the superposition of two flows like shown in Fig. 5(a) (bottom) and (d). Note that the distance between two laser spots is about 110.7 μm. As shown in Fig. 5(a), the left vortex of the top flow and the right one of the middle flow are merged. Thus the region of the jet flows between two remaining vortices becomes wider as the distance between the two laser spots on electrode A increases, since horizontal components of velocity for the interior vortices cancel out but vertical components superpose to a stronger one. Varying the distance between the two laser spots can control the width of the jet flow region. When the two laser spots are sufficiently apart away, it is expected that four vortices can be generated but this was not demonstrated. On the other hand, as two laser spots get closer beyond a certain distance, two interior vortices start to be merged, and consequently the jet flows become faster.

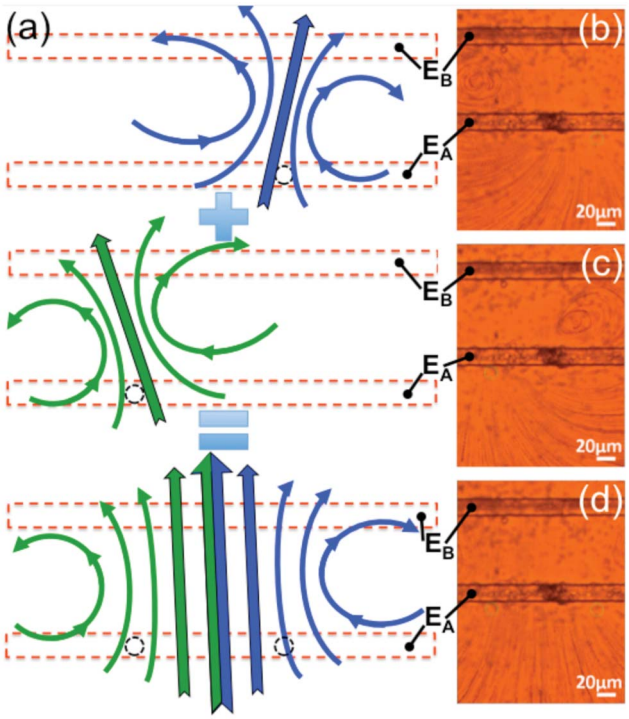

Fig. 5 Twin microvortex generation in milk emulsions. (a) Schematic illustration of superposition of two flows generated by two laser beams. When only one laser spot is located on the right or left side of exposed electrode A (E_A), each flow field is generated shown in (b) or (c). Once two laser spots are simultaneously on exposed electrode A, the superimposed flow is made as shown in (d). The left and right laser spots are located 66.1 μm and 44.6 μm away from the middle of exposed electrode A, respectively. Note that (b), (c), (d) are overlapped images made of 50 frames per each, and show that the middle region of the exposed electrodes (Supplementary movie 5, ESI†).

Conclusions

In conclusion, we have experimentally shown that a new technique can generate various flows with TOMVs using IR illumination as well as optically modified AC electric fields in the microchannel, which is fast, stable, dynamic, and tunable. Also, these opto-electrokinetic flows can be superposed constructively or destructively. Thus this technique is a very promising method to produce a variety of *in situ* fluid flows with shining multiple laser beams as well as one or two laser beams on two coplanar ITO electrodes, which can even manipulate chemical and biological fluids at microscale. On the other hand, further investigation of the underlying

mechanism, especially the interaction between the IR illumination and AC electric fields, is required to increase the feasibility of this technique for transporting, mixing, controlling, and directing fluids.

Acknowledgements

We thank R. Thakur for useful suggestions and C. Smith for supplying ITO glass substrates.

References

1 A. Ramos, H. Morgan, N. G. Green and A. Castellanos, *J. Phys. D: Appl. Phys.*, 1998, **31**, 2338.
2 N. G. Green, A. Ramos, A. Gonzalez, H. Morgan and A. Castellanos, *Phys. Rev. E*, 2000, **61**, 4011.
3 N. G. Green, A. Ramos, A. Gonzalez, A. Castellanos and H. Morgan, *J. Electrost.*, 2001, **53**, 71.
4 A. B. D. Brown, C. G. Smith and A. R. Renniez, *Phys. Rev. E*, 2001, **63**, 016305.
5 M. Z. Bazant and Y. Ben, *Lab Chip*, 2006, **6**, 1455.
6 K. Yang and J. Wu, *Biomicrofluidics*, 2008, **2**, 024101.
7 J. Wu, M. Lian and K. Yang, *Appl. Phys. Lett.*, 2007, **90**, 234103.
8 D. Lastochkin, R. Zhou, P. Wang, Y. Ben and H.-C. Chang, *J. Appl. Phys.*, 2004, **96**, 1730.
9 H. A. Pohl, *Dielectrophoresis*, Cambridge University Press, Cambridge U. K., 1978.
10 N. G. Green, H. Morgan and J. J. Milner, *J. Biochem. Biophys. Methods*, 1997, **35**, 89.
11 N. G. Green and H. Morgan, *J. Phys. D: Appl. Phys.*, 1998, **31**, L25.
12 R. C. Hayward, D. A. Saville and I. A. Aksay, *Nature*, 2000, **404**, 56.
13 P. Y. Chiou, A. T. Ohta and M. C. Wu, *Nature*, 2005, **436**, 370.
14 A. Ashkin, J. M. Dziedzic, J. E. Bjorkholm and S. Chu, *Opt. Lett.*, 1986, **11**, 288.
15 D. G. Grier, *Nature*, 2003, **424**, 810.
16 A. Mizuno, M. Nishioka, Y. Ohno and L. D. Dascalescu, *IEEE Trans. Ind. Appl.*, 1995, **31**, 464.
17 M. Nakano, S. Katsura, G. G. Touchard, K. Takashima and A. Mizuno, *IEEE Trans. Ind. Appl.*, 2007, **43**, 232.
18 G. I. Taylor, *Proc. R. Soc. London, Ser. A*, 1934, **146**, 501.
19 S. J. Williams, A. Kumar and S. T. Wereley, *Lab Chip*, 2008, **8**, 1879.
20 A. Kumar, S. J. Williams and S. T. Wereley, *Microfluid. Nanofluid.*, 2009, **6**, 637.
21 M. Nakano, H. Kurita, J. Komatsu, A. Mizuno and S. Katsura, *Appl. Phys. Lett.*, 2006, **89**, 133901.
22 J. G. Santiago, S. T. Wereley, C. D. Meinhart, D. J. Beebe and R. J. Adrian, *Exp. Fluids*, 1998, **25**, 316.
23 A. Castellanos, A. Ramos, A. Gonzalez, N. G. Green and H. Morgan, *J. Phys. D: Appl. Phys.*, 2003, **36**, 2584.
24 N. G. Green, A. Ramos, A. Gonzalez, H. Morgan and A. Castellanos, *Phys. Rev. E*, 2002, **66**, 026305.
25 R. Hart, R. Lec and H. M. Noh, *Sens. Actuators, B*, 2010, **147**, 366.
26 C.-H. Chen, C.-P. Liu, Y.-C. Lee, F.-B. Hsiao, C.-Y. Chiu, M.-H. Chung and M.-H. Chiang, *J. Micromech. Microeng.*, 2006, **16**, 1463.
27 O. Yavas and M. Takai, *J. Appl. Phys.*, 1999, **85**, 4207.
28 C.-H. Chuang, Y.-W. Huang and Y.-T. Wu, *Sensors*, 2011, **11**, 11021.
29 F. Arai, C. Ng, H. Maruyama, A. Ichikawa, H. El-Shimy and T. Fukuda, *Lab Chip*, 2005, **5**, 1399.
30 E. J. G. Peterman, F. Gittes and C. F. Schmidt, *Biophys. J.*, 2003, **84**, 1308.
31 Microchem SU-8 product data sheet, http://www.microchem.com.
32 J. Oh, R. Hart, J. Capurroa and H. Noh, *Lab Chip*, 2009, **9**, 62.
33 S. Gangwal, O. J. Cayre and O. D. Velev, *Langmuir*, 2008, **24**, 13312.

